Further Simulation Results for "Outage Constrained Robust Transmit Optimization for Multiuser MISO Downlinks: Tractable Approximations by Conic Optimization"

Technical Report

Kun-Yu Wang[⋆], Anthony Man-Cho So[†], Tsung-Hui Chang[‡], Wing-Kin Ma[§], and Chong-Yung Chi[⋆]

February 22, 2014

[⋆]Institute of Communications Engineering, National Tsing Hua University, Hsinchu, Taiwan 30013, R.O.C.
E-mail: kunyuwang7@gmail.com; cychi@ee.nthu.edu.tw.
[†]Department of Systems Engineering and Engineering Management and, by courtesy, the CUHK-BGI Innovation Institute of Trans-omics, The Chinese University of Hong Kong, Hong Kong. E-mail: manchoso@se.cuhk.edu.hk.
[‡]Department of Electronic and Computer Engineering, National Taiwan University of Science and Technology, Taipei 10607, Taiwan, (R.O.C.). E-mail: tsunghui.chang@ieee.org.
[§]Department of Electronic Engineering, The Chinese University of Hong Kong, Hong Kong.
E-mail: wkma@ieee.org.

Abstract— This technical report serves to provide further simulation results for the paper "Outage constrained robust transmit optimization for multiuser MISO downlinks: Tractable approximations by conic optimization". In addition to the rate constrained formulation, which is the main focus of the aforementioned main manuscript, we also demonstrate how the proposed methods can be used to tackle the max-min fairness formulation and the achievable rate region characterization problem.

1 Introduction

In [1], we developed three convex restriction methods for robust outage constrained transmit optimization under the multiuser MISO downlink scenario. Simulation results were provided to illustrate the performance accuracies of the proposed methods. In this technical report, we further demonstrate the efficacy of the proposed methods by showing more simulation results. In particular, we will illustrate the applications of the proposed methods to the max-min fairness formulation and the achievable rate region characterization problem—which was not considered in [1] owing to the limit of space.

2 Further Simulation Results

We follow the simulation results section in the main paper [1] to continue to show more simulation results. The simulation setups for the examples below are generally the same as those in the main paper; the details will not be repeated here and please see Section VI in [1].

2.1 Actual QoS Satisfaction Probabilities

Recall that the three proposed methods, as well as the benchmarked probabilistic SOCP method [2], are conservative in the sense that the rate outage constraints, or the SINR satisfaction probability constraints, are automatically satisfied. In this simulation example, we are interested in examining the gaps between the system's SINR satisfaction probability specification and the actual SINR satisfaction probabilities. In the process, we will also illustrate that the perfect-CSI-based design suffers from severe SINR outages. The simulation settings are the same as those in Simulation Example 1 in [1]. In particular, note that the outage probability requirement is $\rho = 0.1$, i.e., 90% or higher chance of satisfying the SINR requirements. We evaluate the histograms of the actual SINR satisfaction probabilities over different channel realizations. To obtain the histograms, we generated 500 realizations of the presumed channels $\{\bar{\boldsymbol{h}}_i\}_{i=1}^K$. Then, for each channel realization, the actual SINR satisfaction probabilities of all methods were numerically evaluated using $10,000$ randomly generated realizations of the CSI errors $\{\boldsymbol{e}_i\}_{i=1}^K$, which should be sufficient in terms of the probability evaluation accuracy.

Figure 1 shows the histograms obtained. It validates that our proposed methods (and the existing probabilistic SOCP method) indeed adhere to the 90% SINR satisfaction specification. There are two interesting observations, as can be seen from the figure. The first is with the non-robust method. While the non-robust method is, by nature, expected to violate the SINR outage specification, its actual SINR satisfaction probabilities are below 50% for most of the channel realizations, which is severe. This reveals that the perfect-CSI-based design can be quite sensitive to CSI errors. The second is with the conservatism of the various robust methods. The probabilistic SOCP method has its actual SINR satisfaction probabilities concentrating at 100%, which indicates that it may be playing too safe in meeting the outage specification. By contrast, our proposed methods seem to be less conservative. Particularly, among the three methods, Method II (Bernstein-type inequality) appears to be the most relaxed as observed from its histogram. This is consistent with the previous simulation results [1].

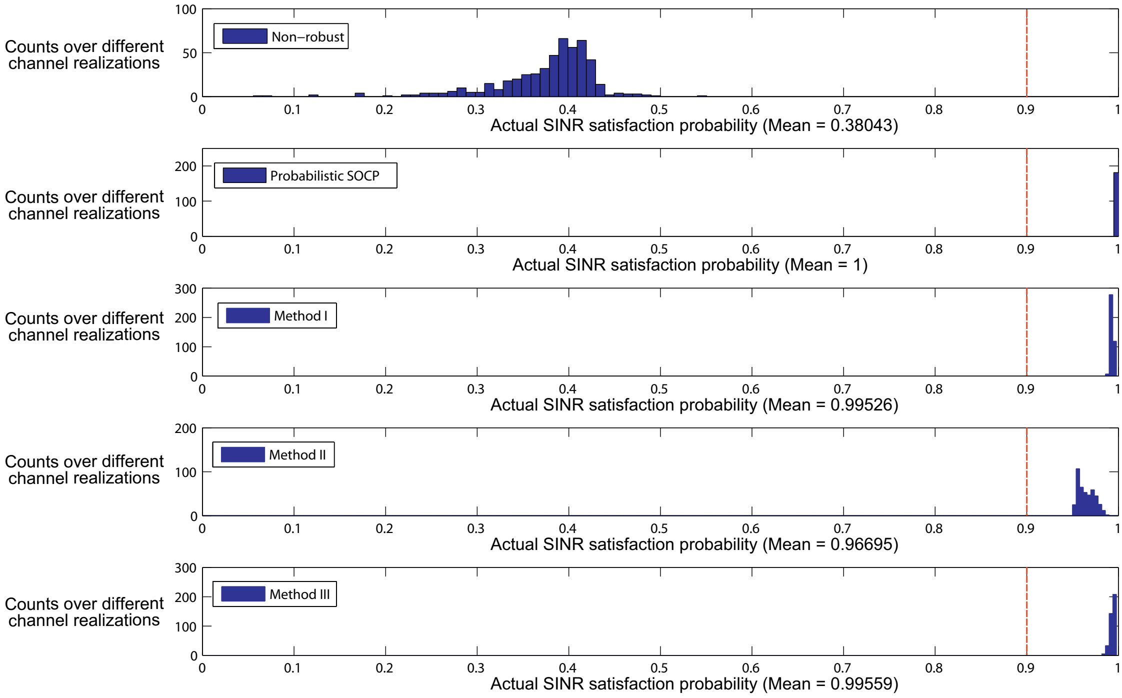

Figure 1: Histograms of the actual SINR satisfaction probabilities of various methods. $N_t = K = 3$; $\boldsymbol{C}_1 = \cdots = \boldsymbol{C}_K = 0.002\boldsymbol{I}_{N_t}$; $\gamma = 11$ dB; $\rho = 0.1$.

2.2 Using the Proposed Methods to Tackle the Max-Min Fairness Formulation

The main paper [1] concentrated only on the rate constrained formulation. In fact, the proposed methods may also be applied to other design formulations. In this simulation example, we consider the application of the proposed methods to the max-min fairness (MMF) formulation.

The MMF formulation aims at finding the largest common rate, say, denoted by r, at which all users' achievable rates are guaranteed to be at least r subject to the total transmission power constraint. In the outage constrained context, we may formulate the MMF problem as

$$\max_{\substack{r\in\mathbb{R},\\ \boldsymbol{S}_1,\ldots,\boldsymbol{S}_K\in\mathbb{H}^{N_t}}} \quad r \tag{1a}$$

$$\text{s.t. } \text{Prob}_{\boldsymbol{h}_i\sim\mathcal{CN}(\bar{\boldsymbol{h}}_i,\boldsymbol{C}_i)}\{\mathsf{R}_i \geq r\} \geq 1-\rho_i, \quad i=1,\ldots,K, \tag{1b}$$

$$\sum_{i=1}^{K} \text{Tr}(\boldsymbol{S}_i) \leq P, \tag{1c}$$

$$\boldsymbol{S}_1,\ldots,\boldsymbol{S}_K \succeq \boldsymbol{0},\ r\geq 0, \tag{1d}$$

where the constant P specifies the system's maximum total transmission power. In the perfect CSI case, it is well known that the MMF problem can be solved via a bisection search strategy [3]. In essence, bisection search utilizes the rate constrained problem as a sub-solver to iteratively find the optimal MMF rate r; for details, please see the literature such as [3, 4]. Here, we adopt the same idea to handle the outage constrained MMF problem (1). Algorithm 1 gives a pseudo-code description of the bisection method. Note that in the algorithm, the rate constrained problems arising in the bisection search are the same rate outage constrained problem we dealt with in the main paper—and thus can be directly handled by the proposed convex restriction methods.

Algorithm 1 Bisection method for the outage constrained MMF problem (1).

1: Given upper and lower bounds $r_{\max}$, $r_{\min}$, and a desired solution accuracy $\epsilon > 0$.
2: **repeat**
3: Set $r = (r_{\min} + r_{\max})/2$.
4: Use one of the proposed convex restriction methods (see Table I in [1]) to approximately solve the following rate outage constrained problem

$$\begin{aligned}\min_{\boldsymbol{S}_1,\ldots,\boldsymbol{S}_K\in\mathbb{H}^{N_t}} \quad & \sum_{i=1}^{K}\text{Tr}(\boldsymbol{S}_i)\\ \text{s.t. } & \text{Prob}_{\boldsymbol{h}_i\sim\mathcal{CN}(\bar{\boldsymbol{h}}_i,\boldsymbol{C}_i)}\{\mathsf{R}_i \geq r\} \geq 1-\rho_i, \quad i=1,\ldots,K,\\ & \boldsymbol{S}_1,\ldots,\boldsymbol{S}_K \succeq \boldsymbol{0},\end{aligned}$$

and set $(\hat{\boldsymbol{S}}_1,\ldots,\hat{\boldsymbol{S}}_K)$ as the corresponding solution.
5: Compute the corresponding total power $\hat{P} = \sum_{i=1}^{K}\text{Tr}(\hat{\boldsymbol{S}}_i)$.
6: Set $r_{\min} = r$ if $\hat{P} \leq P$; otherwise, set $r_{\max} = r$.
7: **until** $r_{\max} - r_{\min} \leq \epsilon$
8: Output r as the achieved MMF rate, and $(\hat{\boldsymbol{S}}_1,\ldots,\hat{\boldsymbol{S}}_K)$ as the corresponding solution.

Let us show some simulation results for the aforementioned outage constrained MMF method. The simulation settings are: $N_t = K = 8$, $\rho = 0.1$, $P = 15$dB, $\boldsymbol{C}_1 = \cdots = \boldsymbol{C}_K = \sigma_e^2\boldsymbol{I}_{N_t}$. Figure 2(a) shows the MMF rates achieved by application of the three proposed convex restriction methods,

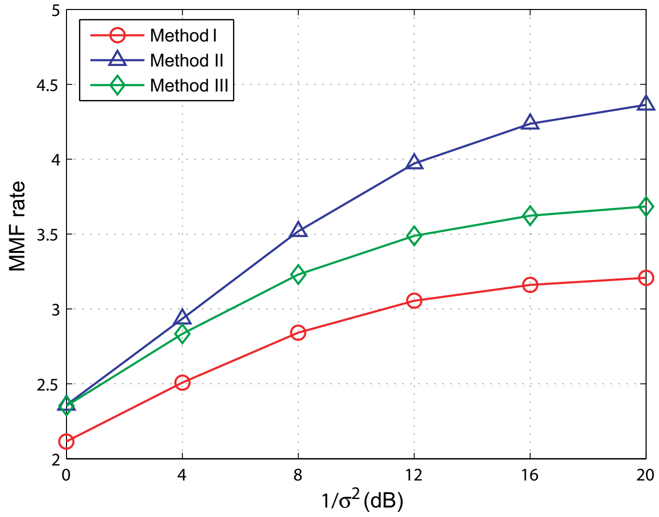

(a)

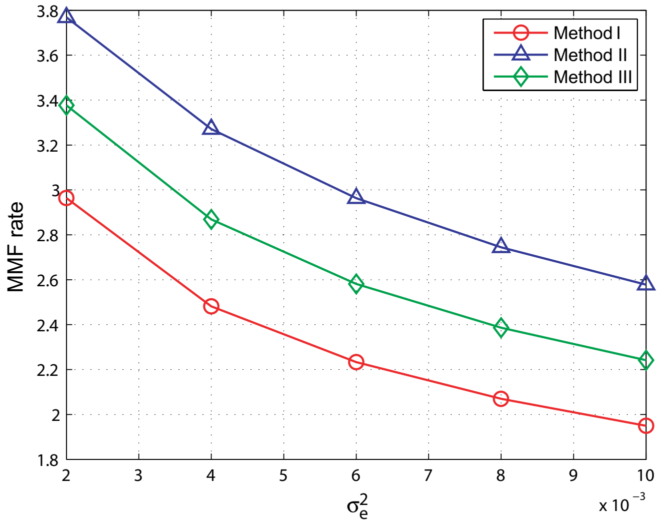

(b)

Figure 2: MMF rate performance of the various methods. (a) MMF rates versus $1/\sigma^2$, with $\sigma_e^2 = 0.002$. (b) MMF rates versus the CSI error level σ_e^2, with $\sigma^2 = 0.1$. $N_t = K = 8$; $\rho = 0.1$; $P = 15$dB.

wherein the MMF rates are plotted against the reciprocal of the noise power (or, roughly speaking, the system's SNR level). We see similar performance trends as in the previous simulation results; in particular, Method II is the best in its MMF rates achieved. Figure 2(b) shows the MMF rates w.r.t. the CSI uncertainty level. Again, similar performance behaviors are observed.

2.3 Using the Proposed Methods to Perform Rate Region Characterization

The proposed methods may also be used to evaluate the achievable rate region. In the outage constrained context, the achievable rate region may be expressed as

$$\mathcal{R} = \bigcup_{\substack{\boldsymbol{S}_1,\ldots,\boldsymbol{S}_K \succeq \boldsymbol{0}, \\ \sum_{i=1}^K \mathrm{Tr}(\boldsymbol{S}_i) \leq P}} \left\{ (r_1,\ldots,r_K) \succeq \boldsymbol{0} \ : \ \mathrm{Prob}_{\boldsymbol{h}_i \sim \mathcal{CN}(\bar{\boldsymbol{h}}_i, \boldsymbol{C}_i)} \{ \mathsf{R}_i \geq r_i \} \geq 1 - \rho_i, i = 1,\ldots,K \right\} \quad (2)$$

where $P > 0$ is the maximum total transmission power. We are interested in characterizing $\mathcal{R}$ by determining its Pareto boundary. Such a problem can be handled by the rate-profile approach [5, 6], previously developed for the perfect CSI case. To describe how the approach works in the outage constrained case, let us first introduce a *rate-profile problem* for the achievable rate region defined in (2):

$$r^\star(\boldsymbol{\alpha}) = \max_{\substack{r \in \mathbb{R}, \\ \boldsymbol{S}_1,\ldots,\boldsymbol{S}_K \in \mathbb{H}^{N_t}}} \ r \quad \text{(3a)}$$

$$\text{s.t. } \mathrm{Prob}_{\boldsymbol{h}_i \sim \mathcal{CN}(\bar{\boldsymbol{h}}_i, \boldsymbol{C}_i)} \{ \mathsf{R}_i \geq \alpha_i \cdot r \} \geq 1 - \rho_i, \quad i = 1,\ldots,K, \quad \text{(3b)}$$

$$\sum_{i=1}^K \mathrm{Tr}(\boldsymbol{S}_i) \leq P, \quad \text{(3c)}$$

$$\boldsymbol{S}_1,\ldots,\boldsymbol{S}_K \succeq \boldsymbol{0}, \ r \geq 0, \quad \text{(3d)}$$

where $\boldsymbol{\alpha} = (\alpha_1,\ldots,\alpha_K) \succeq \boldsymbol{0}$, $\sum_{i=1}^K \alpha_i = 1$, is given and is called a *rate-profile vector*. It is known that a Pareto optimal point of $\mathcal{R}$ can be obtained by solving problem (3) with respect to a particular $\boldsymbol{\alpha}$, and then evaluating the corresponding rate-tuple $(\alpha_1 r^\star(\boldsymbol{\alpha}),\ldots,\alpha_K r^\star(\boldsymbol{\alpha}))$ [5, 6]. Hence, the Pareto boundary of $\mathcal{R}$ may be characterized by solving problem (3) for different $\boldsymbol{\alpha}$'s. To solve problem (3), we note that problem (3) takes almost the same form as the MMF problem (1). For this reason, every rate-profile problem can be processed by the same bisection method described in the previous subsection (with minor modifications).

Some simulation demonstrations are given as follows. We consider a two-user scenario ($K = 2$), and set $N_t = 2$, $P = 15$dB, $\rho = 0.1$, $\sigma^2 = 0.1$, $\boldsymbol{C}_1 = \cdots = \boldsymbol{C}_K = \sigma_e^2 \boldsymbol{I}_{N_t}$, $\sigma_e^2 = 0.002$. Figure 3(a) shows the outage constrained achievable rate regions obtained by the three proposed convex restriction methods; the probabilistic SOCP method is also included for comparison. As seen from the figure, the rate regions yielded by the three proposed methods are better than that by the probabilistic SOCP method. Also, Method II outperforms both Methods I and III, and Method I works better than Method III. Figure 3(b) shows another rate region result where we increase N_t to 8. The results look similar, except that Method III is better than Method I this time.

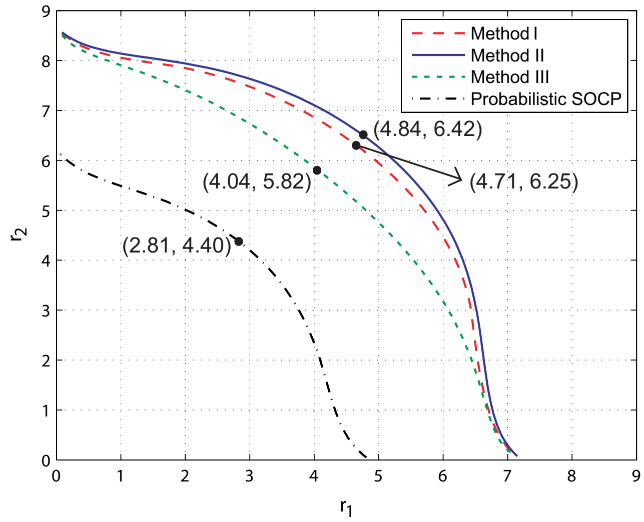

(a)

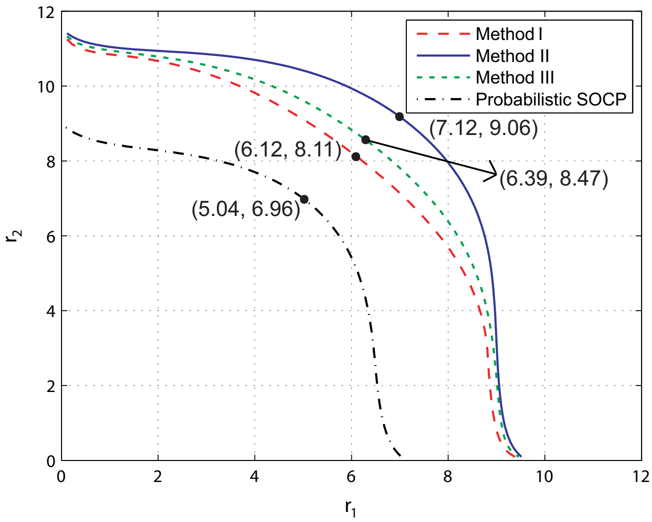

(b)

Figure 3: Rate regions obtained by various methods. (a) $N_t = K = 2$. (b) $N_t = 8$, $K = 2$. The solid circles indicate the sum-rate maximization points.

Acknowledgments

This work is supported in part by the National Science Council, R.O.C., under Grant NSC-102-2221-E-007-019-MY3 and Grant NSC-102-2221-E-011-005-MY3; in part by the Hong Kong Research Grants Council (RGC) General Research Fund (GRF), under Project CUHK 416012; in part by The Chinese University of Hong Kong, under Direct Grant 2050506; in part by the Shun Hing Institute of Advanced Engineering at The Chinese University of Hong Kong, under Project #MMT-p2-09.

References

[1] K.-Y. Wang, A. M.-C. So, T.-H. Chang, W.-K. Ma, and C.-Y. Chi, "Outage constrained robust transmit optimization for multiuser MISO downlinks: Tractable approximations by conic optimization," *submitted to IEEE Trans. Signal Process.*, 2014.

[2] M. B. Shenouda and T. N. Davidson, "Probabilistically-constrained approaches to the design of the multiple antenna downlink," in *Proc. 42nd Asilomar Conference 2008*, Pacific Grove, October 26-29, 2008, pp. 1120–1124.

[3] A. Wiesel, Y. C. Eldar, and S. Shamai, "Linear precoding via conic optimization for fixed MIMO receivers," *IEEE Trans. Signal Process.*, vol. 54, no. 1, pp. 161–176, Jan. 2006.

[4] S. Boyd and L. Vandenberghe, *Convex Optimization.* Cambridge, U.K.: Cambridge Univ. Press,, 2004.

[5] M. Mohseni, R. Zhang, and J. M. Cioffi, "Optimized transmission for fading multiple-access and broadcast channels with multiple antennas," *IEEE Journal on Sel. Areas in Commun.*, vol. 24, no. 8, pp. 1627–1639, Aug. 2006.

[6] R. Zhang and S. Cui, "Cooperative interference management with MISO beamforming," *IEEE Trans. Signal Process.*, vol. 58, no. 10, pp. 5450–5458, 2010.